JOURNAL OF PROTEOMICS 115 (2015) 117–131

Available online at www.sciencedirect.com

ScienceDirect

www.elsevier.com/locate/jprot

Transcriptome and proteome analysis of *Eucalyptus* infected with *Calonectria pseudoreteaudii*

Quanzhu Chen[a], *Wenshuo Guo*[b,c,*], *Lizhen Feng*[b,c], *Xiaozhen Ye*[c], *Wanfeng Xie*[c], *Xiuping Huang*[c], *Jinyan Liu*[c]

[a]*Sanming City Forest Disease and Pest Control and Quarantine Station, Sanming, Fujian 365000, China*
[b]*Forestry College, Fujian Agriculture and Forestry University, Fuzhou 350002, China*
[c]*Institute of Forestry Protection, Fujian Agriculture and Forestry University, Fuzhou, 350002, China*

ARTICLE INFO

Article history:
Received 5 July 2014
Accepted 12 December 2014

Keywords:
Eucalyptus
Cylindrocladium leaf blight
Defense pathways
Defense related gene
iTRAQ
RNA-seq

ABSTRACT

Cylindrocladium leaf blight is one of the most severe diseases in *Eucalyptus* plantations and nurseries. There are *Eucalyptus* cultivars with resistance to the disease. However, little is known about the defense mechanism of resistant cultivars. Here, we investigated the transcriptome and proteome of *Eucalyptus* leaves (*E. urophylla* × *E. tereticornis* M1), infected or not with *Calonectria pseudoreteaudii*. A total of 8585 differentially expressed genes ($|\log_2$ ratio$| \geq 1$, FDR ≤ 0.001) at 12 and 24 hours post-inoculation were detected using RNA-seq. Transcriptional changes for five genes were further confirmed by qRT-PCR. A total of 3680 proteins at the two time points were identified using iTRAQ technique.The combined transcriptome and proteome analysis revealed that the shikimate/phenylpropanoid pathway, terpenoid biosynthesis, signalling pathway (jasmonic acid and sugar) were activated. The data also showed that some proteins (WRKY33 and PR proteins) which have been reported to involve in plant defense response were up-regulated. However, photosynthesis, nucleic acid metabolism and protein metabolism were impaired by the infection of *C. pseudoreteaudii*. This work will facilitate the identification of defense related genes and provide insights into *Eucalyptus* defense responses to *Cylindrocladium* leaf blight.

Biological significance
In this study, a total of 130 proteins and genes involved in the shikimate/phenylpropanoid pathway, terpenoid biosynthesis, signalling pathway, cell transport, carbohydrate and energy metabolism, nucleic acid metabolism and protein metabolism in *Eucalyptus* leaves after infected with *C. pseudoreteaudii* were identified. This is the first report of a comprehensive transcriptomic and proteomic analysis of *Eucalyptus* in response to *Calonectria* sp.

1. Introduction

Eucalyptus species and their clones have been extensively developed in China in recent decades due to their fast growth rate and favourable wood properties. There are many diseases caused by a wide range of pathogens in commercial *Eucalyptus* plantations and nurseries [1,2]. *Cylindrocladium* leaf blight (CLB) is regarded as one of the most serious ones. In China,

* *Corresponding author at:* Forestry College, Fujian Agriculture and Forestry University, Fuzhou 350002, China. Tel./fax: +86 591 83799336.
E-mail address: fjgws@126.com (W. Guo).

http://dx.doi.org/10.1016/j.jprot.2014.12.008
1874-3919/

CLB was first found in 1992 in Guangdong Province. It was later found in Guangxi, Fujian, and Hainan, in that order. CLB is caused by *Calonectria* sp., especially their anamorph form, *Cylindrocladium* [3–5]. There are several *Calonectria* species in Fujian, including *C. pauciramosa*, *C. crousiana*, *C. fujianensis* *C. pseudocolhounii*, *C. pseudoreteaudii* and *C. kyotensis*. Of these, *C. pseudoreteaudii* is one of the most virulent ones in both *Eucalyptus* plantations and nurseries [3,4]. CLB is often characterized by leaf blotch and shoot blight, even defoliation and mortality, which can significantly decrease productivity. Annual economic losses due to this disease in Fujian alone are estimated to be over $ 7.8 million [6]. It really threatens the long term sustainability of *Eucalyptus* plantations.

There are rich germplasm resources of *Eucalyptus* in Fujian, and several of them, for example, *E. urophylla* × *E. tereticornis* M1, are resistant to *Calonectria* sp. [7]. But molecular mechanism of *Eucalyptus* defense against the infection of *Calonectria* sp. is still far from being understood. To date, studies have been limited mostly to the perspectives of morphology and physiochemistry. The issue has only rarely been addressed on a genetic level, and it has never been investigated at the protein level. With respect to morphology and physiochemistry, scholars have selected some important morphological and physiochemical indices for early identification of disease resistance [2,8–13]. On the genetic level, only one suppression subtractive hybridization cDNA library has been constructed, for *E. grandis* × *E. urophylla* 9224 induced by *C. quinqueseptatum* Morgan [14]. Some up-regulated genes were identified. Of these, 23 genes with known function were involved in signal transduction, plant resistance response, photosynthesis, energy transfer, protein metabolism, and plant growth.

So far, large-scale transcriptional and proteomic profiling of the plant response to microorganisms have been always performed in *Arabidopsis thaliana* and other model plants, but rarely in *Eucalyptus* [15]. Transcriptional profiling based on total RNA sequencing (RNA-seq) is a powerful tool for analyzing gene expression changes in respond to various environmental stresses. RNA-seq uses next generation sequencing technology to sequence and quantify transcripts, and can provide detailed and systematic changes of gene expression involved in plant defenses against microorganisms. Since the expression of some genes is regulated at the translational level, proteome analysis is required for deeply understanding the defense mechanism. Isobaric tags for relative and absolute quantification (iTRAQ) is a new protein quantification technology based on isotope labeling combined with multidimensional liquid chromatography and tandem mass spectrometry (LC-MS/MS) [16]. It has been widely applied in various areas of life science for its high sensitivity and accuracy.

With the recently releasing of *E. grandis* genome, *Eucalyptus* transcriptome and proteome profiling will become important methodologies for studies of *Eucalyptus* defense mechanism [17]. In this study, parallel analysis of transcriptome and proteome of *E. urophylla* × *E. tereticornis* M1 infected or not with *C. pseudoreteaudii* were performed by RNA-seq and iTRAQ technologies. *E. grandis* genome was used as the reference sequence (Phytozome 7.0, 2011). qRT-PCR was used to validate the RNA-seq data and evaluate whether the observed responses of the resistant clone to *Calonectria* also occur on the susceptible clone. The aim of this study was to identify a set of candidate defence genes and pathways associated with CLB resistance.

2. Materials and methods

2.1. Plant materials and *C. pseudoreteaudii* inoculation

The resistant clone *E. urophylla* × *E. tereticornis* M1 and the susceptible clone *E. grandis* No.5, were employed as experimental materials. The tissue-cultured seedlings of *Eucalyptus* were cultivated in the nursery of Fujian Agriculture and Forestry University, Fuzhou, Fujian Province, China.Uniform plants (about 25 cm in height) for each clone were selected and grown in a climate chamber with 25–28 °C, 90% humidity and a 14 h/10 h (day/night) photoperiod on 5th May 2012. Leaves of each clone were evenly sprayed with a spore suspension (2.0×10^5 condia · mL^{-1}) of *C. pseudoreteaudii* strain YA5j2 until run-off at 9:00 am in June 30th, 2012. The strain YA5j2 was isolated from *Eucalyptus* leaves which showed typical symptoms of leaf blight and cultured on potato dextrose agar [4]. The spore suspension was prepared as Feng et al. [14]. For mock-inoculation, plants of the same clone were inoculated in a similar fashion with sterile water. For transcriptome and proteome analysis, ten individual plants of the resistant clone were used to treat. For each individual plant, two leaves were collected at 12 and 24 h post-inoculaiton (hpi). For functional test, leaves of the resistant clone and the susceptible clone were collected from different plants but with the same treatments at 0, 24 and 60 hpi. The leaves were immediately frozen in liquid nitrogen, and then stored at −80 °C until RNA and protein extraction.

2.2. RNA isolation, illumina sequencing and raw data processing

Total RNA was extracted from mixed leaves of ten replications of each sample using RNAplant Plus Reagent DP437 (Tiangen, Beijing, China) according to the manufacturer's instructions. The concentration and quality of RNA were determined using an Agilent 2100 Bioanalyzer (Agilent Technologies, Santa Clara, CA, USA).

Total RNA extracts were then sent to the Beijing Genomics Institute for RNA-Seq analysis (BGI, Shenzhen, China). The construction of the cDNA library and sequencing were performed as previous report [18,19]. Briefly, mRNA of "*E. urophylla* × *E. tereticornis* M1" was enriched using the oligo(dT) magnetic beads. Adding the fragmentation buffer, the mRNA was interrupted to short fragments (about 200 bp), then the first strand cDNA was synthesized by random hexamer-primer using the mRNA fragments as templates. Buffer, dNTPs, RNase H and DNA polymerase I were added to synthesize the second strand. The double strand cDNA was purified with QiaQuick PCR Purification Kit (Qiagen, Germany) and washed with EB buffer for end repair and single nucleotide A (adenine) addition. Finally, sequencing adaptors were ligated to the fragments. The required fragments was purified by agrose gel electrophoresis and enriched by PCR amplification. The library products were ready for sequencing analysis via Illumina HiSeq™ 2000 (Illumina, San Diego, CA, USA).

The resulting data were analyzed in a slightly modified version of the procedure as previous description [18]. Clean reads of each sample were mapped to the sequenced genome of *E. grandis* (http://phytozome.net/eucalyptus.php)

using SOAPaligner/soap2 software allowing two base mismatches [20].

The gene expression level is calculated by using RPKM method (Reads Per kb per Million reads) [21], and the formula is shown as follows:

$$RPKM = \frac{10^6 C}{NL/10^3}$$

Given RPKM(A) to be the expression of gene A, C to be number of reads that uniquely aligned to gene A, N to be total number of reads that uniquely aligned to all genes, and L to be number of bases on gene A. The RPKM method is able to eliminate the influence of different gene length and sequencing discrepancy on the calculation of gene expression. Therefore, the calculated gene expression can be directly used for comparing the difference of gene expression among samples. If there is more than one transcript for a gene, the longest one is used to calculate its expression level and coverage. Gene coverage is the percentage of a gene covered by reads. This value is equal to the ratio of the base number in a gene covered by unique mapping reads to the total bases number of that gene.

2.3. Identification and annotation of DEGs

Differentially expressed genes (DEGs) in the two stages between pathogen-inoculated and mock-inoculated samples were identified referring to Audic [22].

Denote the number of unambiguous clean tags from gene A as x, given every gene's expression occupies only a small part of the library, p(x) will closely follow the Poisson distribution.

$$p(x) = \frac{e^{-\lambda}\lambda^x}{x!} (\lambda \text{ is the real transcripts of the gene})$$

The total clean tag number of the sample 1 is N1, and total clean tag number of sample 2 is N2; gene A holds × tags in sample1 and y tags in sample 2. The probability of gene A expressed equally between two samples can be calculated with:

$$2\sum_{i=0}^{i=y} p(i|x)$$

$$\text{Or } 2 \times \left(1 - \sum_{i=0}^{i=y} p(i|x)\right)\left(\text{if} \sum_{i=0}^{i=y} p(i|x) > 0.5\right)$$

$$p(y|x) = \left(\frac{N_2}{N_1}\right)^y \frac{(x+y)!}{x!y!\left(1+\frac{N_2}{N_1}\right)^{(x+y+1)}}$$

p-Value corresponds to differential gene expression test. FDR (False Discovery Rate) is a method to determine the threshold of *p*-value in multiple tests. Assume that we have picked out R differentially expressed genes in which S genes really show differential expression and the other V genes are false positive. If we decide that the error ratio "Q = V/R" must stay below a cutoff (e.g. 1%), we should preset the FDR to a number no larger than 0.01. In this paper, "FDR ≤ 0.001 and the absolute value of log2Ratio ≥ 1" were set as the threshold to judge the significance of gene expression difference.

Then, all DEGs were mapped to gene ontology terms in the database (GO, http://www.geneontology.org/) for functional annotation. Additionally, the DEGs were subjected to Kyoto Encyclopedia of Genes and Genomes database (KEGG, http://www.genome.jp/kegg/pathway.html) enrichment analysis to identify the main metabolic pathways and signal transduction pathways of DEGs using Blastall software [23].

2.4. Quantitative reverse transcription-PCR

qRT-PCR was used to validate the data of RNA-Seq and to evaluate whether the observed defense responses of the resistant clone to *Calonectria* also occur on the susceptible clone.

About 2 μg total RNA was used for cDNA synthesis by Rever Tra Ace qPCR RT Kit (Toyobo, Osaka, Japan) according to the manufacturers' instructions. The specific primers for each selected gene were designed with Primer Software Version 5.0 (PREMIER Biosoft International, CA, USA) and synthesized by GenScript (Nanjing) Co., Ltd. The primer sequences are shown in Supplemental Table S1. PCR amplification was conducted in a 20 μl reaction system containing 10 μl SYBR® Green Realtime PCR Master Mix (Toyobo, Osaka, Japan) and performed on a LightCycler 480 II Real-Time PCR System (Roche Applied Science, Mannheim, Germany). The cycling conditions were 95 °C for 30 s followed by 45 cycling of 95 °C for 5 s, 60 °C for 10 s and 72 °C for 15 s. Six replicates (three biological replicates × two technical replicates) were performed for each target gene. *Actin 2* (Eucgr.I00241.1) and *Transcript elongation factor IIS* (Eucgr.A00774.1) were used as the reference genes [24]. The relative expression levels of target genes were analyzed using the $2^{-\Delta\Delta CT}$ method [25].

2.5. Protein extraction and iTRAQ reagent labeling

The plant materials used for iTRAQ analysis were the same as those for RNA-Seq. Protein was extracted from each sample according to the method of Yang et al. [26]. The protein concentration and quality were determined using a Protein Assay Kit (Bio-Rad, Hercules, CA, USA) and confirmed with a 15% SDS-PAGE (Geneview, USA).

iTRAQ analysis was carried out as previous reports at Beijing Genomics Institute (BGI, Shenzhen, China) [26]. Brief, After adjusting the pH to 8.5 with 1 M ammonium bicarbonate, total protein from each sample was reduced for 1 h at 56 °C by adding DTT to 10 mM, and alkylated with 55 mM iodoacetamide for 45 min at room temperature in the dark. Trypsin (Promega, USA) was then added to a final substrate/enzyme ratio of 20:1 (w/w). The digest was incubated at 37 °C for overnight. A total of four samples were then labeled using iTRAQ Reagent-8plex Multiplex Kit according to the manufacturer's instructions (Applied Biosystems, Foster City, CA, USA). Two pathogen-inoculated samples were labeled with iTRAQ tags 113 and 115, two control samples labeled with tags 117 and 119.

2.6. Strong cation-exchange fractionation

The labeled samples were mixed and lyophilized. They were then resuspended in 4 mL of solvent A (25% v/v acetonitrile, 25 mM NaH_2PO_4, pH 2.7) and loaded into a Ultremex SCX column (4.6 × 250 mm) (Shimadzu LC-20AB HPLC). The peptide

was eluted at 1 mL · min^{-1} using solvent A for 10 min, 5-35% solvent B (25 mM NaH_2PO_4, 1 M KCl, 25% v/v acetonitrile, pH 2.7) for 11 min, and then 35-80% solvent B for 1 min. The eluted fractions were monitored through a UV detector at 214 nm. Fractions were collected every 1 min, and consecutive fractions with low peak intensity were combined. A total of twenty fractions were obtained, desalted using a Strata X C18 column (Phenomenex, USA) and then vacuum-dried.

2.7. Liquid chromatography–mass spectrometry (LC–MS/MS)

Each of the dried fractions was dissolved with solvent C (5% v/v acetonitrile, 0.1% Formic acid) and centrifuged at 20,000 g for 10 min. The final concentration was 0.5 μg/μl. The peptide (8 μl) was loaded into a 2 cm C18 trap column (inner diameter 200 μm) on an Shimadzu LC-20 AD nano HPLC. The sample was loaded at 8 μl/min for 4 min, then eluted at 300 nl/min for 40 min with a gradient of 2-35% solvent D (95% v/v acetonitrile, 0.1% Formic acid), followed by a 5 min linear gradient to 80%, maintaining at 80% solvent D for 4 min, and then solvent C for 1 min.

The eluted peptides were analyzed using nanoelectrospray ionization followed by tandem mass spectrometry (MS/MS) in an Q-Exactive (Thermo Fisher Scientific,San Jose,USA) coupled online to the HPLC. Intact peptides were detected in the Orbitrap with a resolution of 70,000. Peptides were selected for MS/MS using higher energy collision dissociation (HCD) operating mode with a normalized collision energy setting of 27 %. A data-dependent procedure that alternated between one MS scan followed by fifteen MS/MS scans was applied for the three most abundant precursorions above a threshold ion count of 20,000 in the MS survey scan.

2.8. Data analysis

The MS spectra were analyzed by a thorough search using Mascot software (version 2.3.02, Matrix Science Inc., Boston, MA) against *E. grandis* database (JGI version 0.9, www.phytozome.org/Egrandis, 46,315 sequences). Search parameters were as followed: MS/MS ion search; trypsin enzyme; fragment mass tolerance 0.02 Da; monoisotopic mass values; variable modifications of Gln- > pyro-Glu (N-term Q), oxidation (M) and iTRAQ8plex (Y); peptide mass tolerance 15 ppm; one max missed cleavage. To reduce false positive results, all data were reported based on a 95% confidence and false discovery rate (FDR) less than 1%. For quantitative analysis, a protein must have at minimum one unique peptide matches with iTRAQ ratios. A 1.2-fold cutoff value was used to identify up-regulated and down-regulated proteins with a *p*-value of less than 0.05.

3. Results

3.1. Inoculation and symptom development

Leaves of *E. urophylla* × *E. tereticornis* M1 were inoculated with the spore suspension of *C. pseudoreteaudii* and mock-inoculated with sterile water. No visible symptoms were observed at 12 hpi (Supplemental Fig. S1). Typical symptoms appeared at 24 hpi and were exacerbated at 60 hpi.

3.2. RNA sequencing and mapping

To identify differentially expressed genes (DEGs) that respond to *C. pseudoreteaudii* in *E. urophylla* × *E. tereticornis* M1, expression profiles of *Eucalyptus* leaves at 12 and 24 h after *C. pseudoreteaudii*-inoculation and mock-inoculation were investigated using a RNA-Seq technique. A total of 29 303 637 high quality reads were obtained from the four samples (Table 1). For each sample, 74 –82% of the reads could be mapped to the genome of *E. grandis*; of these mapped reads, 58–69% matched uniquely. And 51–59% of the reads could be mapped to the gene of *E. grandis*; of these mapped reads, 30 – 36% matched uniquely.

3.3. Identification of DEGs

The statistical analysis of gene expression were shown in Supplementary Table 2 in [27]. Based on a FDR ≤ 0.001 and |log2 Ratio| ≥ 1, a total of 8585 (3203 up-regulated and 5382 down-regulated) DEGs were detected at the two time points after inoculation with *C. pseudoreteaudii*. More down-regulated genes than up-regulated genes were observed at all time points. Of the up-regulated genes, 2018 genes were detected at both time points; 464 genes were expressed only at 12 hpi and 721 genes were expressed only at 24 hpi (Fig. 1). Of the down-regulated genes, 3775 were observed at the both points in time. 699 genes were down-regulated only at 12 hpi, and 908 only at 24 hpi (Fig. 1).

Among the DEGs with |log2 Ratio| ≥ 15, more up-regulated genes (50) than down-regulated genes (4) were detected at 12 hpi, while 68 up-regulated genes and 50 down-regulated genes were found at 24 hpi (Supplemental Table S2). Of these genes, several were found to associate with stress reponse or phytohormone signalling. For example, a MLP-like protein 423 gene (Eucgr.A00133.1) was strongly induced at both of the time points, and a glutathione S-transferase gene (Eucgr.F02915.1) was highly expressed at 24 hpi. Besides that, lots of new transcripts and hypothetical proteins were detected in our data. Further study could be performed on these new genes and unknown function genes.

To evaluate the gene expression profile, 5 genes including 3 up-regulated genes and 2 down-regulated genes at the two time points were selected to perform qRT-PCR (Fig. 2). The results showed that the expression patterns of all genes were the same as the RNA-seq results, despite some differences in the expression level. It indicated that the RNA-seq results are reliable.

KEGG pathway analysis was further carried out to understand the main biological pathways affected by the infection of *C. pseudoreteaudii*. Twenty pathways that showed the smallest Q value at each time point were selected, in which zeatin biosynthesis, limonene and pinene degradation, photosynthesis, stilbenoid, diarylheptanoid and gingerol biosynthesis, porphyrin and chlorophyll metabolism, linoleic acid metabolism showed significant enrichment at all time points (Q ≤ 0.05) (Fig. 3). While photosynthesis - antenna proteins, terpenoid backbone biosynthesis, glutathione metabolism, and plant circadian rhythm presented significant enrichment at 12 hpi, ABC transporters, flavonoid biosynthesis, galactose metabolism were significantly enriched at 24 hpi.

Table 1 – Reads mapping to the genome and gene of *Eucalyptus grandis*.

		C1		C2		T1		T2	
		read number	percentage	read number	percentage	read number	percentage	read number	percentage
Map to Genome	Total Reads	7043306	100.00%	7390699	100.00%	7478902	100.00%	7390730	100.00%
	Total Mapped Reads	5487015	77.90%	5496519	74.37%	6078963	81.28%	5921850	80.13%
	perfect match	3197389	45.40%	3185260	43.10%	3608933	48.25%	3466771	46.91%
	<=3 bp mismatch	2289626	32.51%	2311259	31.27%	2470030	33.03%	2455079	33.22%
	unique match	4769909	67.72%	4327817	58.56%	5151915	68.89%	4946308	66.93%
	multi-position match	717106	10.18%	1168702	15.81%	927048	12.40%	975542	13.20%
	Total Unmapped Reads	1556291	22.10%	1894180	25.63%	1399939	18.72%	1468880	19.87%
Map to Gene	Total Reads	7043306	100.00%	7390699	100.00%	7478902	100.00%	7390730	100.00%
	Total Mapped Reads	3834710	54.44%	3822395	51.72%	4411633	58.99%	4176915	56.52%
	perfect match	2492351	35.39%	2422836	32.78%	2851485	38.13%	2694706	36.46%
	<=2 bp mismatch	1342359	19.06%	1399559	18.94%	1560148	20.86%	1482209	20.05
	unique match	2168679	30.79%	2334275	31.58%	2634057	35.22%	2484644	33.62%
	multi-position match	1666031	23.65%	1488120	20.14%	1777576	23.77%	1692271	22.90%
	Total Unmapped Reads	3208596	45.56%	3568304	48.28%	3067269	41.01%	3213815	43.48%

C1 and C2 represent the mock-inoculated leaves at 12 and 24 hours, respectively; T1 and T2 represent the *C. pseudoreteaudii*-inoculated leaves at 12 and 24 hours, respectively.

3.4. Proteomics characterization by iTRAQ

In order to complement the transcriptome analysis, proteomes were surveyed at the same two points in time using iTRAQ technique, and a total of 3680 proteins were identified and listed in Supplementary Table 3 in [27]. A 95% confidence level ($P < 0.05$) and a 1.2-fold change were used to identify proteins that were differentially expressed between *C. pseudoreteaudii*-inoculated leaves and mock-inoculated leaves. Using these criteria, 406 differentially expressed proteins (254 up-regulated and 152 down-regulated) at 12 hpi and 225 (142 up-regulated and 83 down-regulated) at 24 hpi were detected at the two time points. A summary of differentially abundant proteins was presented in Supplementary Table 4 in [27]. In addition, a comparison between the proteome data and their transcriptome data resulted in a total of 130 proteins whose expression patterns were consistant with the transcriptional level (Table 2). Of these, four proteins couldn't be observed at 12 hpi both at protein level and transcript level, and six proteins couldn't be observed at 24 hpi both at protein level and

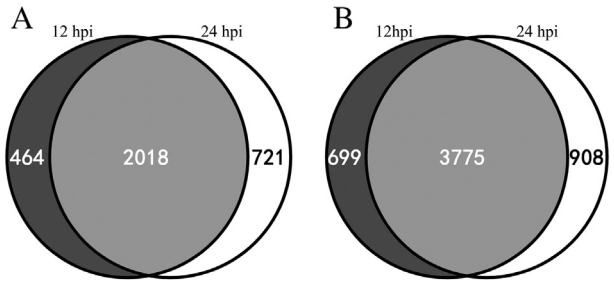

Fig. 1 – Venn diagrams showing common differential expressed genes. Common significantly up-regulated genes (A) and down-regulated genes (B) with a cut-off of $|\log_2$ Ratio$| \geq 1$ and *P*-value ≤ 0.05 in *E. urophylla* × *E. tereticornis* M1 between 12 and 24 h post-inoculation with *C. pseudoreteaudii*.

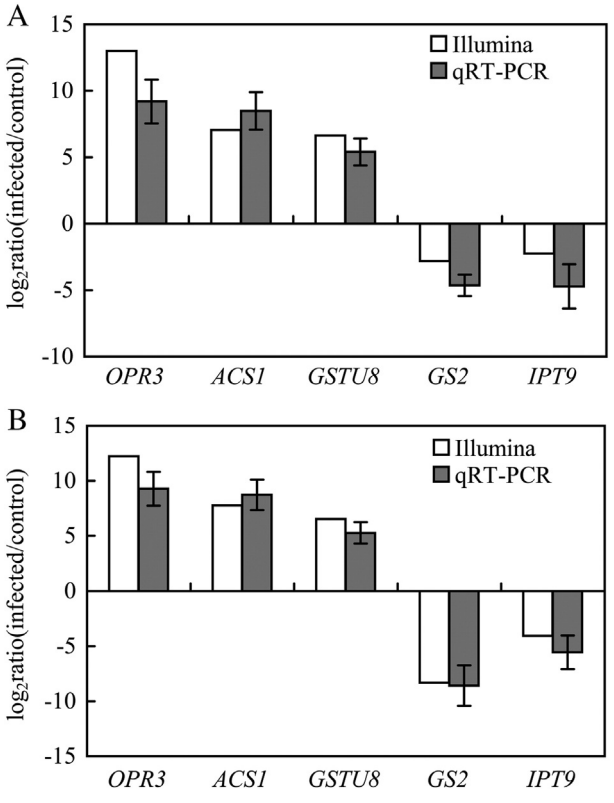

Fig. 2 – Validation of DEGs by qRT-PCR analysis. The relative expression levels of five differential expressed genes in "*E. urophylla* × *E. tereticornis* M1" at 12 and 24 h post-inoculation with *C. pseudoreteaudii* were obtained by RNA-seq using RPKM method (white) and by qRT-PCR using the $2^{-\Delta\Delta CT}$ method (black). Bars represent mean ± SE (n = 6). *OPR3*, oxophytodienoate-reductase 3; *ACS1*, 1-aminocyclopropane-1-carboxylic acid synthase 1; *GSTU8*, glutathione S-transferase TAU 8; *GS2*, glutamine synthetase 2; *IPT9*, isopentenyltransferase 9.

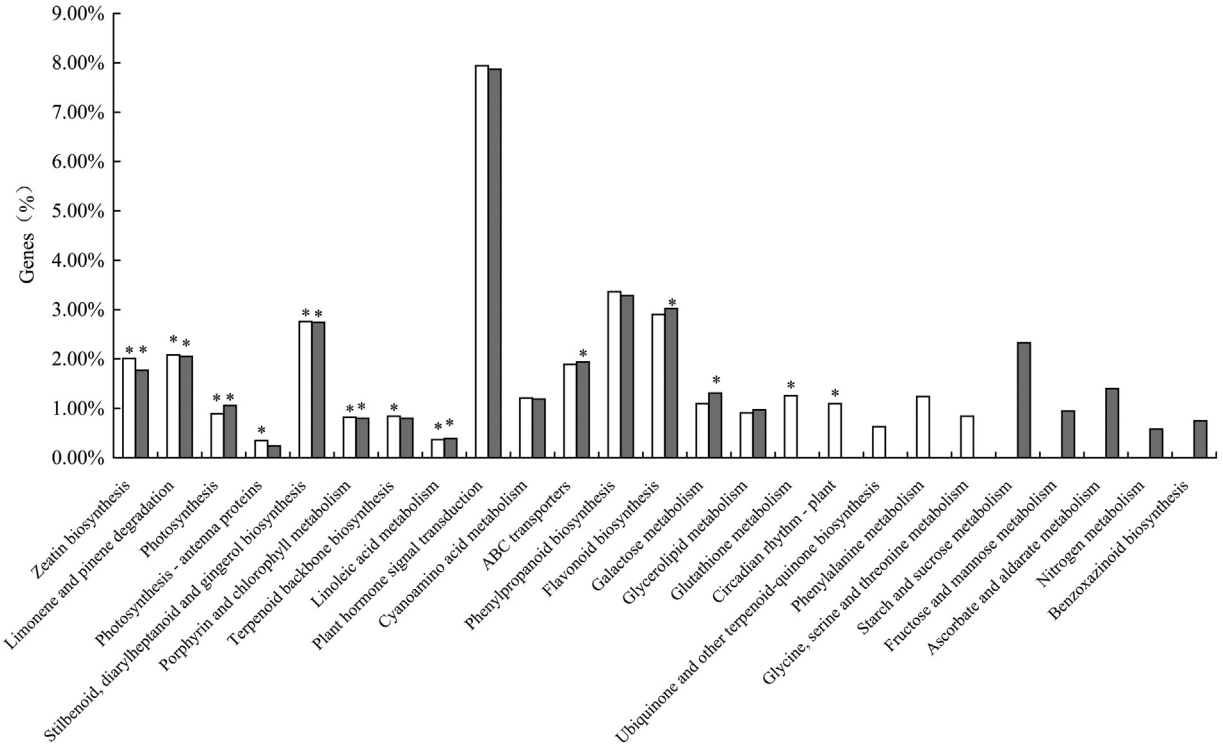

Fig. 3 – KEGG pathway enrichment analysis of differential expressed genes. Twenty pathways that show the smallest Q value were selected at 12 hpi (white)and 24 hpi (black). * represents the significant enriched pathways (Q ≤ 0.05).

transcript level. It indicated that these proteins may play role only at 12 hpi or 24 hpi. 48 proteins couldn't be detected at protein level at 12 hpi, and 42 proteins couldn't be detected at protein level at 24 hpi. It implied that these proteins translated more lately.

KEGG pathway analysis was also performed to investigate the main biological pathways which the differentially expressed proteins enriched (Fig. 4). Together with the transcriptome data, several significantly enriched pathways were found, including phenylalanine metabolism, flavonoid biosynthesis at 12 hpi, and terpenoid backbone biosynthesis, linoleic acid metabolism, galactose metabolism, stilbeno,diarylheptanoid, gingerol biosynthesis, flavonoid biosynthesis at 24 hpi. These pathways have been reported to involve in stress response both directly and indirectly [28].

3.5. *Comparison of response pathways between the resistant clone and the susceptible clone*

To evaluate whether the observed signal transduction and defence-related pathways to *Calonectria* were specific responses in the resistant clone, expression levels of a set of genes belonging to different biological pathways were investigated in both the resistant clone (*E. urophylla* × *E. tereticornis* M1) and the susceptible clone (*E. grandis* No.5) at 0, 24 and 60 hpi using qRT-PCR (Fig. 5). The results showed that most of these genes were also differentially expressed in the susceptible clone except for *LRR-RLK* (Eucgr.F01306.1). It should be noted, however, the differentially expression patterns in the susceptible clone were different from those in the resistant clone. The susceptible outcome may attribute to the lack or the lower expression, or the delayed activation of some genes required to overcome the pathogen.

4. Discussion

In this study, the transcriptome and proteome difference between *C. pseudoreteaudii*-inoculated *Eucalyptus* leaves and mock-inoculated leaves at the two time points were investigated by RNA-Seq and iTRAQ technologies, respectively. RNA-Seq analysis revealed that a total of 8585 genes were differentially expressed at 12 hpi and 24 hpi. Proteome analysis identified 3680 proteins, in which 406 and 225 proteins were found to be differentially expressed at 12 hpi and 24 hpi, respectively. Among these proteins, only 130 demonstrated the same differentially expression patterns as the transcript levels (Table 2). A poor correlation has been reported to be a normal phenomenon for several reasons, such as posttranscriptional, translational, and posttranslational regulatory processes. This may be also for the reason that the present detecting technology of gene is far more mature than the one of protein.The main pathways of these proteins and their genes will be discussed in the next part.

4.1. *Stress responses*

4.1.1. *Shikimate/phenylpropanoid pathway*

One of the most remarkable changes that took place in *E. urophylla* × *E. tereticornis* M1 after *C. pseudoreteaudii* infection was that most of the enzymes involved in the shikimate/phenylpropanoid pathway and its branches were up-regulated,

Table 2 – Differential expression proteins and their corresponding genes by iTRAQ and RNA-seq.

Gene model	Homology in *Arabidopsis thaliana*	*A. thaliana* annotation	12 hpi		24 hpi	
			protein [a]	gene [b]	protein [a]	gene [b]
Stress responses						
Eucgr.K02940.1	AT2G38470.1	WRKY DNA-binding protein 33	1.733	4.876	2.267	4.814
Eucgr.H03995.1	AT1G24020.1	MLP-like protein 423	1.568	4.527	1.862	4.662
Eucgr.H04013.3	AT1G24020.1	MLP-like protein 423	-	1.839	1.51	1.639
Eucgr.H04003.1	AT1G24020.1	MLP-like protein 423	-	2.530	1.513	2.522
Eucgr.H04007.1	AT1G24020.1	MLP-like protein 423	1.295	2.497	2.024	2.480
Eucgr.H04010.1	AT1G24020.1	MLP-like protein 423	1.412	2.382	1.987	2.452
Eucgr.H04019.1	AT1G24020.1	MLP-like protein 423	1.508	1.542	1.695	2.762
Eucgr.A00125.1	AT1G24020.1	MLP-like protein 423	-	-	14.346	14.832
Eucgr.J01079.1	AT3G53260.1	phenylalanine ammonia-lyase 2	2.423	4.276	4.45	4.035
Eucgr.F00366.2	AT1G22410.1	Class-II DAHP synthetase family protein	1.468	4.527	2.906	4.735
Eucgr.I00519.1	AT4G39980.1	3-deoxy-D-arabino-heptulosonate 7-phosphate synthase 1	-	-	1.261	1.136
Eucgr.D02465.1	AT2G45300.1	5-enolpyruvylshikimate 3-phosphate synthase	1.244	2.082	-	1.840
Eucgr.C02284.1	AT1G51680.1	4-coumarate:CoA ligase 1	1.792	3.438	2.95	3.859
Eucgr.H03920.1	AT5G54160.1	O-methyltransferase 1	2.122	3.196	2.446	4.237
Eucgr.J01844.1	AT2G30490.1	cinnamate-4-hydroxylase	1.906	2.711	2.208	2.514
Eucgr.G01417.1	AT4G34050.1	CCoAOMT1 S-adenosyl-L-methionine-dependent methyltransferases superfamily protein	1.608	4.251	3.267	4.200
Eucgr.G02088.1	AT1G68040.1	S-adenosyl-L-methionine-dependent methyltransferases superfamily protein	1.316	2.483	2.048	1.533
Eucgr.J03126.1	AT5G48930.1	hydroxycinnamoyl-CoA shikimate/quinate hydroxycinnamoyl transferase	-	4.214	2.908	4.484
Eucgr.F03816.1	AT3G55120.1	Chalcone-flavanone isomerase family protein	0.766	−2.812	-	−3.815
Eucgr.D01931.1	AT4G11820.2	hydroxymethylglutaryl-CoA synthase / HMG-CoA synthase / 3-hydroxy-3-methylglutaryl coenzyme A synthase	-	2.889	1.739	2.656
Eucgr.J00991.1	AT3G54250.1	GHMP kinase family protein	1.235	3.052	1.855	3.654
Eucgr.A01783.1	AT3G02780.1	isopentenyl pyrophosphate/dimethylallyl pyrophosphate isomerase 2	-	1.979	1.314	2.004
Eucgr.E03836.1	AT5G47770.1	farnesyl diphosphate synthase 1	-	2.022	1.388	2.645
Eucgr.F01453.1	AT5G36110.1	cytochrome P450, family 716, subfamily A, polypeptide 1(CYP716A)	1.835	1.990	2.357	1.289
Eucgr.B04037.1	AT5G24910.1	cytochrome P450, family 714, subfamily A, polypeptide 1	-	2.994	3.816	2.851
Eucgr.C00059.1	AT5G36110.1	cytochrome P450, family 716, subfamily A, polypeptide 1(CYP716A)	-	3.129	2.163	2.809
Eucgr.L01417.1	AT3G09270.1	glutathione S-transferase TAU 8	1.203	5.662	1.352	5.042
Eucgr.A01555.1	AT3G52960.1	Thioredoxin superfamily protein	0.802	−1.916	-	−2.639
Eucgr.C00774.1	AT3G26060.1	Thioredoxin superfamily protein	0.694	−3.528	-	−6.362
Eucgr.H00830.1	AT4G28730.1	Glutaredoxin family protein	0.819	−1.670	-	−1.808
Eucgr.J00880.1	AT1G50320.1	thioredoxin X	-	−4.804	0.826	−3.135
Eucgr.F04229.1	AT1G76760.1	thioredoxin Y1	1.529	1.466	1.256	-
Eucgr.L02460.1	AT2G41480.1	Peroxidase superfamily protein	2.253	4.258	2.137	1.647
Eucgr.I02271.1	AT3G12500.1	ATHCHIB,B-CHI,CHI-B,HCHIB,PR-3,PR3 basic chitinase	0.444	−1.517	0.52	−5.409
Eucgr.I02395.1	AT5G66400.1	ATDI8,RAB18 Dehydrin family protein	0.704	−1.814	-	-
Eucgr.I02606.1	AT2G14170.1	aldehyde dehydrogenase 6B2	0.733	−2.223	-	−1.965
Eucgr.B00357.1	AT3G48000.1	aldehyde dehydrogenase 2B4	0.805	−3.119	-	−5.278
Eucgr.F03543.1	AT1G20510.1	OPCL1 OPC-8:0 CoA ligase1	0.693	−1.340	-	−1.818
Eucgr.J00836.1	AT5G13000.1	glucan synthase-like 12	-	−2.100	0.805	−1.843
Eucgr.H03539.1	AT4G02050.1	sugar transporter protein 7	2.715	5.966	3.342	5.809
Eucgr.F03137.1	AT3G13784.1	cell wall invertase 5	-	2.456	1.579	3.214
Eucgr.F03138.1	AT3G13784.1	cell wall invertase 5	-	3.273	1.625	3.749
Eucgr.C00201.1	AT2G18700.1	trehalose phosphatase/synthase 11	1.865	4.143	-	4.466
Eucgr.C03563.1	AT5G12080.1	mechanosensitive channel of small conductance-like 10	-	4.840	1.45	3.794
Eucgr.D01804.1	AT2G46150.1	Late embryogenesis abundant (LEA) hydroxyproline-rich glycoprotein family	-	3.519	1.835	3.497
Eucgr.A00617.1	AT3G51660.1	Tautomerase/MIF superfamily protein	-	−4.602	0.703	−14.744
Eucgr.F00208.1	AT5G67090.1	Subtilisin-like serine endopeptidase family protein	-	−4.475	0.667	−3.976
Eucgr.F01795.2	AT1G20810.1	FKBP-like peptidyl-prolyl cis-trans isomerase family protein	0.785	−1.557	-	−6.174
Eucgr.E04322.1	AT5G45680.1	FK506-binding protein 13	0.83	−3.043	-	−7.004
Eucgr.I00717.1	AT5G67400.1	root hair specific 19	-	3.499	1.366	2.983
Eucgr.H02622.1	AT1G23820.1	spermidine synthase 1	-	2.226	1.398	1.526
Eucgr.E02950.1	AT2G15490.3	UDP-glycosyltransferase 73B4		4.401	2.919	3.310
Eucgr.I00055.1	AT3G06650.1	ATP-citrate lyase B-1	-	2.442	1.669	2.772

(continued on next page)

Table 2 (*continued*)

Gene model	Homology in *Arabidopsis thaliana*	*A. thaliana* annotation	12 hpi		24 hpi	
			protein [a]	gene [b]	protein [a]	gene [b]
Signal transduction						
Eucgr.F00761.1	AT3G20410.1	calmodulin-domain protein kinase 9	1.485	2.648		2.234
Eucgr.F01306.1	AT1G53430.1	Leucine-rich repeat transmembrane protein kinase	-	2.327	1.471	2.938
Eucgr.I01368.1	AT4G38810.2	Calcium-binding EF-hand family protein	0.706	−3.580	-	−1.967
Eucgr.B03570.1	AT5G61790.1	calnexin 1	1.715	1.804	1.219	2.041
Eucgr.C01068.1	AT4G13350.1	(nuclear shuttle protein)-interacting GTPase	-	1.096	1.314	1.437
Eucgr.K02102.1	AT3G07390.1	AIR12 auxin-responsive family protein	0.683	−3.280	-	−3.196
Eucgr.F01505.1	AT5G42650.1	allene oxide synthase	1.316	3.593	2.041	2.782
Eucgr.H04495.1	AT1G55020.1	lipoxygenase 1	-	1.967	1.246	2.283
Eucgr.J00821.1	AT3G45140.1	lipoxygenase 2	-	3.268	2.307	2.260
Eucgr.L01891.1	AT3G45140.1	lipoxygenase 2	-	6.074	3.374	6.439
Cell transport						
Eucgr.B03603.1	AT5G19760.1	Mitochondrial substrate carrier family protein	1.227	1.114	-	1.701
Eucgr.C02092.1	AT2G24520.1	H(+)-ATPase 5	-	1.732	1.26	1.133
Eucgr.D02276.1	AT4G11610.1	calcium/lipid-binding plant phosphoribosyltransferase family protein	-	1.738	1.35	1.428
Eucgr.H02886.1	AT4G13510.1	ammonium transporter 1;1	-	2.071	1.521	1.630
Eucgr.E03242.1	AT5G46110.2	Glucose-6-phosphate/phosphate translocator-related	0.679	−2.808	-	−4.384
Eucgr.K01911.1	AT5G06530.1	ABC-2 type transporter family protein	-	−3.477	0.471	−4.948
Eucgr.A01832.1	AT4G28390.1	ADP/ATP carrier 3	3.559	5.123	4.026	6.164
Eucgr.G03388.1	AT5G13490.1	ADP/ATP carrier 2	2.161	1.466	-	1.720
Eucgr.G03387.1	AT5G13490.1	ADP/ATP carrier 2	-	2.273	1.225	2.029
Carbohydrate and energy metabolism						
Eucgr.I00200.1	AT5G64040.2	photosystem I reaction center subunit PSI-N, chloroplast, putative	0.269	−3.813	-	−16.062
Eucgr.J02958.1	AT1G52230.1	photosystem I subunit H2	0.814	−3.981	-	−3.312
Eucgr.F03038.1	AT3G16140.1	photosystem I subunit H1	0.69	−3.074	-	−4.566
Eucgr.E02381.1	AT2G34430.1	light-harvesting chlorophyll-protein complex II subunit B1	-	-	1.756	2.849
Eucgr.D00322.1	AT2G34430.1	light-harvesting chlorophyll-protein complex II subunit B1	0.785	−3.098	-	-
Eucgr.G03390.1	AT3G63540.1	Mog1/PsbP/DUF1795-like photosystem II reaction center PsbP family protein	-	−3.024	0.771	−4.781
Eucgr.F04030.1	AT1G78900.1	vacuolar ATP synthase subunit A	0.664	−1.243	-	−1.832
Eucgr.K01354.1	AT1G03475.1	Coproporphyrinogen III oxidase	0.581	−1.759	-	−1.614
Eucgr.B03320.1	AT1G70410.2	beta carbonic anhydrase 4	-	−2.854	0.827	−2.775
Eucgr.I01374.1	AT2G21170.1	triosephosphate isomerase	0.711	−1.978	-	−2.137
Eucgr.E00872.1	AT4G10960.1	UDP-D-glucose/UDP-D-galactose 4-epimerase 5	0.802	−1.040	-	−1.145
Eucgr.C02330.1	AT4G30210.2	AR2,ATR2,P450 reductase 2	2.963	2.679	3.077	2.721
Eucgr.B02637.1	AT1G59960.1	NAD(P)-linked oxidoreductase superfamily protein	-	1.764	1.662	1.552
Eucgr.I00273.1	AT5G05320.1	FAD/NAD(P)-binding oxidoreductase family protein	2.323	8.491	-	7.960
Eucgr.E03807.1	AT4G05020.1	NAD(P)H dehydrogenase B2	-	4.499	1.608	4.361
Eucgr.I02232.1	AT4G35260.1	isocitrate dehydrogenase 1	-	1.565	1.362	1.518
Eucgr.F00458.1	AT1G58280.1	Phosphoglycerate mutase family protein	-	3.142	1.771	3.044
Eucgr.F02441.1	AT1G78060.1	Glycosyl hydrolase family protein	-	−2.455	0.653	−3.915
Eucgr.G00445.1	AT4G34480.1	O-Glycosyl hydrolases family 17 protein	0.81	−2.204	0.765	−2.185
Eucgr.C03896.1	AT4G26140.1	beta-galactosidase 12	0.402	−1.833	-	-
Eucgr.I00108.1	AT5G63810.1	beta-galactosidase 10	0.798	−1.953	0.763	−1.284
Eucgr.F03224.1	AT1G17160.1	pfkB-like carbohydrate kinase family protein	0.65	−2.079	-	-
Eucgr.G01121.1	AT5G09650.1	pyrophosphorylase 6	-	−1.548	0.813	−2.634
Eucgr.A02907.1	AT5G61510.1	GroES-like zinc-binding alcohol dehydrogenase family protein	-	−2.660	0.814	−4.606
Eucgr.K02981.1	AT5G01410.1	Aldolase-type TIM barrel family protein	1.394	1.915	1.257	-
Nucleic acid metabolism						
Eucgr.C00902.1	AT2G19570.1	AT-CDA1,CDA1,DESZ cytidine deaminase 1	1.283	1.279	-	-
Eucgr.A02571.1	AT3G52380.1	chloroplast RNA-binding protein 33	0.825	−3.295	-	−3.889
Eucgr.I02029.1	AT1G74230.1	glycine-rich RNA-binding protein 5	0.604	−1.801	-	−1.486
Eucgr.H02772.1	AT2G18510.1	RNA-binding (RRM/RBD/RNP motifs) family protein	0.634	−1.307	-	−1.094
Eucgr.F04002.1	AT3G21215.1	RNA-binding (RRM/RBD/RNP motifs) family protein	0.746	−1.077	-	−1.131
Eucgr.I02364.2	AT2G18050.1	histone H1-3	0.481	−2.461	0.427	−15.466
Eucgr.K01707.1	AT3G56490.1	HIS triad family protein 3	0.66	−1.177	-	−3.312
Eucgr.J00682.1	AT5G12200.1	pyrimidine 2	0.72	−3.017	-	−3.379

Table 2 (*continued*)

Gene model	Homology in *Arabidopsis thaliana*	*A. thaliana* annotation	12 hpi		24 hpi	
			protein [a]	gene [b]	protein [a]	gene [b]
Protein metabolism						
Eucgr.B03574.1	AT1G26910.1	Ribosomal protein L16p/L10e family protein	1.257	1.409	-	-
Eucgr.D01771.1	AT1G64510.1	Translation elongation factor EF1B/ribosomal protein S6 family protein	0.158	−3.338	-	−4.680
Eucgr.D01115.1	AT2G43030.1	Ribosomal protein L3 family protein	-	−2.143	0.772	−3.089
Eucgr.D02125.1	AT4G17560.1	Ribosomal protein L19 family protein	-	−2.771	0.74	−5.084
Eucgr.F01878.1	AT1G75350.1	Ribosomal protein L31	-	−2.172	0.709	−3.034
Eucgr.E03558.1	ATCG00770.1	ribosomal protein S8	-	-	0.76	−3.077
Eucgr.F02900.1	AT5G17330.1	glutamate decarboxylase	1.295	1.987	-	2.420
Eucgr.H02679.1	AT4G13930.1	serine hydroxymethyltransferase 4	-	2.323	1.33	2.375
Eucgr.I02231.1	AT4G35630.1	phosphoserine aminotransferase	-	4.455	1.694	3.088
Eucgr.H02279.1	AT5G67360.1	ARA12 Subtilase family protein	-	−3.314	0.754	−2.453
Eucgr.A02225.1	AT1G28110.1	serine carboxypeptidase-like 45	-	-	2.535	1.326
Eucgr.K02421.1	AT2G27920.3	serine carboxypeptidase-like 51	0.758	-	0.829	−2.589
Eucgr.H02345.1	AT5G65760.1	Serine carboxypeptidase S28 family protein	-	−2.535	0.813	−3.103
Eucgr.G03227.1	AT5G07030.1	Eukaryotic aspartyl protease family protein	0.755	−5.035	-	−4.951
Eucgr.B02617.1	AT3G18420.1	Protein prenylyltransferase superfamily protein	-	1.777	1.496	1.181
Eucgr.K01508.1	AT5G17920.1	Cobalamin-independent synthase family protein	1.591	2.681	-	2.606
Eucgr.D02028.2	AT1G12250.1	Pentapeptide repeat-containing protein	0.827	−4.450	-	−4.366
Unknown						
Eucgr.K03002.1	AT1G07380.1	Neutral/alkaline non-lysosomal ceramidase	0.517	−1.605	-	−2.360
Eucgr.F03012.1	AT3G16000.1	MAR binding filament-like protein 1	0.744	−3.250	-	−4.664
Eucgr.H00149.1	AT5G43310.2	COP1-interacting protein-related	0.768	−2.741	-	−3.055
Eucgr.F02850.1	AT1G23170.2	Protein of unknown function DUF2359, transmembrane	1.497	1.371	-	1.559
Eucgr.H00206.1	AT3G01680.1		0.617	−2.910	-	−3.353
Eucgr.H00201.1	AT3G01680.1		-	−2.065	0.599	−4.150
Eucgr.H03305.1	AT1G09310.1	Protein of unknown function, DUF538	-	−1.831	0.728	−2.806

- not detected at the gene level or protein level.

[a] Fold-change of differentially expressed proteins in *E. urophylla* × *E. tereticornis* M1 after infection with *C. pseudoreteaudii*.

[b] $\log_2$ Ratio of the genes differentially expressed in *E. urophylla* × *E. tereticornis* M1 after infection with *C. pseudoreteaudii*.

including two 3-deoxy-D-arabino-heptulosonate-7-phosphate synthase (DAHPS), one 5-enolpyruvylshikimate 3-phosphate synthase (EPSPS), one phenylalanine ammonialyase (PAL), one cinnamate-4-hydroxylase (C4H), one 4-coumarate CoA ligase (4CL), one caffeoyl-CoA O-methyltransferase1 (CCoAOMT) , and one hydroxycinnamoyl-CoA shikimate/quinate hydroxycinnamoyltransferase (HCT). qRT-PCR results of this study also illustrated that the expression level of *PAL2* (Eucgr.J01079.1) in the resistant clone reached a peak at 24 hpi, which was earlier than in the suscepitable clone (Fig. 5).

DAHPS is the first enzyme in the shikimate pathway. It catalyzes the conversion of phosphoenolpyruvate (PEP) and D-erythrose 4-phosphate (E4P) to 3-deoxy-D-arabino-heptulosonate-7-phosphate (DAHP) and phosphate. In *Arabidopsis thaliana*, AtDAHPS1 is induced by wounding and pathogen infection [29]. EPSPS is the sixth key enzyme in the shikimate pathway and has received considerable attention ever since it was first found to be the primary target of glyphosate in the 1980s [30]. PAL, C4H, and 4CL are the core enzymes involved in the early stages of phenylpropanoid biosynthesis. PAL catalyzes the conversion of L-phenylalanine to trans-cinnamic acid and ammonia. It is a key enzyme in the regulation of carbon flow into the phenylpropanoid pathway [31]. It can be induced by various stimuli, such as pathogenic attacks, tissue wounding, and hormones [32]. Furthermore, a positive correlation has been observed between PAL activity and phenylpropanoid biosynthesis using PAL mutations and heterologous PAL overexpression [31,33,34]. CCoAOMT and HCT are essential to lignin biosynthesis. Lignin, which is ubiquitous in tracheophytes, is a key structural component of vascular plants [35].

It is estimated that about 20% of all fixed carbon flows through the shikimate pathway under normal conditions [36]. Even more carbon flows through the pathway under stress conditions [29,37]. The phenylpropanoid pathway not only contributes to plant development but also plays a crucial role in plant–microbe interactions [38,39]. It can provide precursors for the synthesis of antimicrobial and structural components, including lignins, salicylates, coumarins, hydroxycinnamic amides, flavonoid phytoalexins, and antioxidants. The up-regulation of shikimate/phenylpropanoid pathway suggested that it may play an important role in *Eucalyptus* defence against *Calonectria*. A previous study also showed that *E. urophylla* × *E. tereticornis* M1 had higher contents of polyphenol and flavonoid than susceptible cultivars after infection by *C. quinqueseptatum* [9]. For example, the contents of polyphenol and flavonoid at 24 hpi were 22.26 % and 10.13 mg · g^{-1} in *E. urophylla* × *E. tereticornis* M1, while 10.15 % and 5.76 mg · g^{-1} in *E. grandis* No.5.

4.1.2. *Terpenoid biosynthesis*

Terpenoids (also named isoprenoids) which are widely distributed in almost all higher plants, consist of a large number of

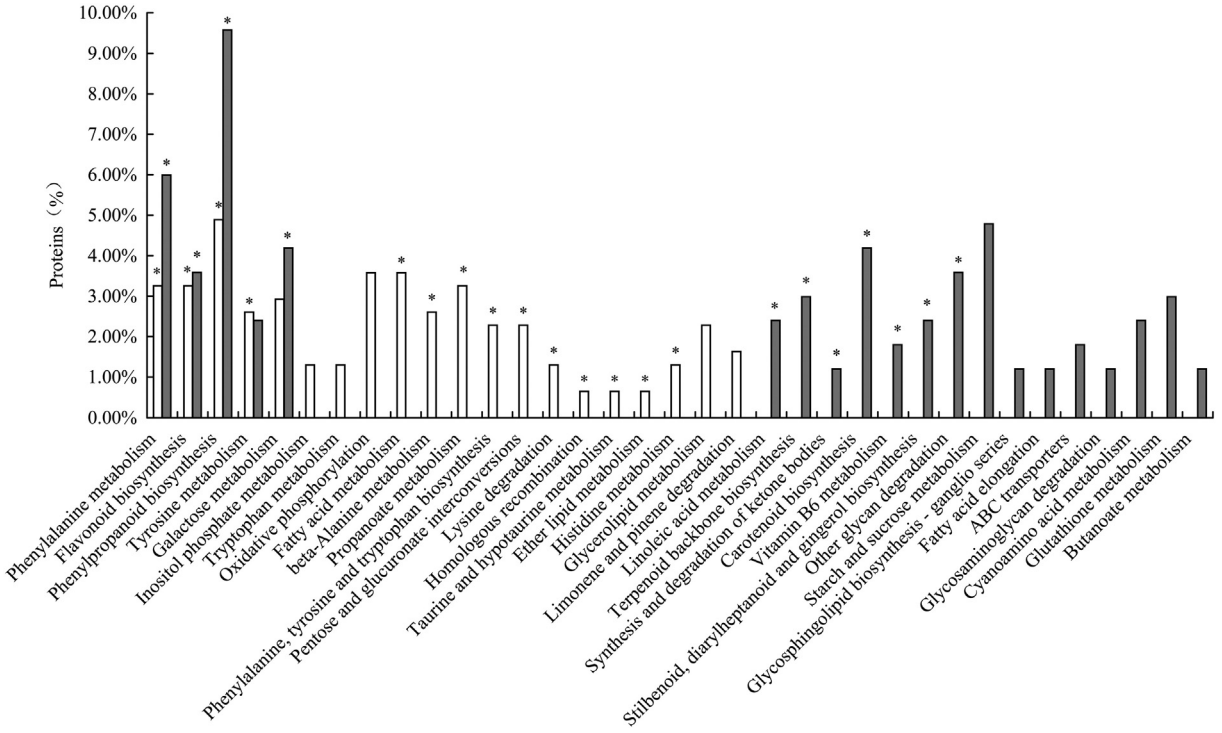

Fig. 4 – KEGG pathway enrichment analysis of differential expressed proteins. Twenty pathways that show the smallest Q value were selected at 12 hpi (white)and 24 hpi (black). * represents the significant enriched pathways (Q ≤ 0.05).

chemical compounds and serve a vital role in plant defense [40]. *Eucalyptus* sp. contain abundant terpenoids, including 1,8-cineole (above 70%),α-terpineol, terpinen-4-ol, linalool, α-pinene, β-pinene, globulol, and epiglobulol [41]. Terpenoids are generated from isopentenyl diphosphate (IPP) and its isomer, dimethylallylpyrophosphate (DMAPP), which can be separately synthesized through the mevalonic acid (MVA) pathway and the methylerythritol phosphate (MEP) pathway. The present data showed that five proteins involved in the synthesis of terpenoids (3-hydroxy-3-methylglutaryl coenzyme A synthase; GHMP kinase family protein; isopentenyl pyrophosphate/dimethylallyl pyrophosphate isomerase 2; farnesyl diphosphate synthase 1; cytochrome P450, family 716, subfamily A, polypeptide 1) were up-regulated. It suggested that the terpenoid pathway may be enhanced in *E. urophylla* × *E. tereticornis* M1 after infection by *C. pseudoreteaudii*. Then the plants may accumulate more terpenoids to resist the pathogen. Similar results were found in *Lactuca* [28]. A foreign gene encoding farnesyl diphosphate synthase in transgenic tobacco was found to enhance resistance to *Alternaria alternata* [42].

4.1.3. ROS scavenging system

Pathogen infection may result in rapid accumulation of reactive oxygen species (ROS) in plants. This causes tissue necrosis, which can increase susceptibility to necrotrophism, but ROS accumulation also induces resistance to biotrophic pathogens [43]. In this way, elevation of antioxidant capacity of plants increases their resistance to cell death induced by necrotrophic pathogens.

C. pseudoreteaudii-inoculated *Eucalyptus* showed changes in the abundances of proteins involved in ROS scavenging. Among them, glutathione S-transferase TAU, thioredoxin Y1, and peroxidase superfamily protein became more abundant, and two thioredoxin superfamily proteins, glutaredoxin family protein and thioredoxin X1 became less so. Peroxidase (POD) functioned in the lignin and suberin biosynthesis and in the regulation of reactive oxygen species (ROS) [54]. *POD* overexpression enhanced plant resistance and silencing plant resulted in an increase in plant susceptibility. qRT-PCR showed that the expression abundance of *POD* (Eucgr.L02460.1) in the resistant clone was higher than in the susceptible clone after infection with *Calonectria* (Fig. 5). A previous study also showed that POD activity after infection by *C. quinqueseptatum* was higher in *E. urophylla* × *E. tereticornis* M1 than in susceptible cultivars [10]. For example, the POD activity at 24 hpi was 5.45 $U \cdot g^{-1}$ (FW) $\cdot min^{-1}$ in *E. urophylla* × *E. tereticornis* M1, while 2.89 $U \cdot g^{-1}$ (FW) $\cdot min^{-1}$ in *E. grandis* No.5. All the data suggested that the effect of *POD* on the resistant clone may be conected to strengthening of the cell wall.

4.1.4. Other defense proteins

In this study, several proteins associated with plant defense were up-regulated, including seven MLP-like proteins and one WRKY transcription factor. MLP-like proteins belonging to the PR-10 protein family were also significantly up-regulated in cotton roots and hypocotyl tissues infected with *Fusarium oxysporum* f. sp. *vasinfectum* [44]. Similarly, Sun et al. showed that MLP-like proteins could be induced in *Panax ginseng* by stress treatment involving light and mannitol [45]. PRs can be regulated by WRKY transcription factors through W-box motif, which binds to WRKY factors, thus activating the plants' defense responses [46]. WRKY33, one of the positive regulators, may have a key role in plant

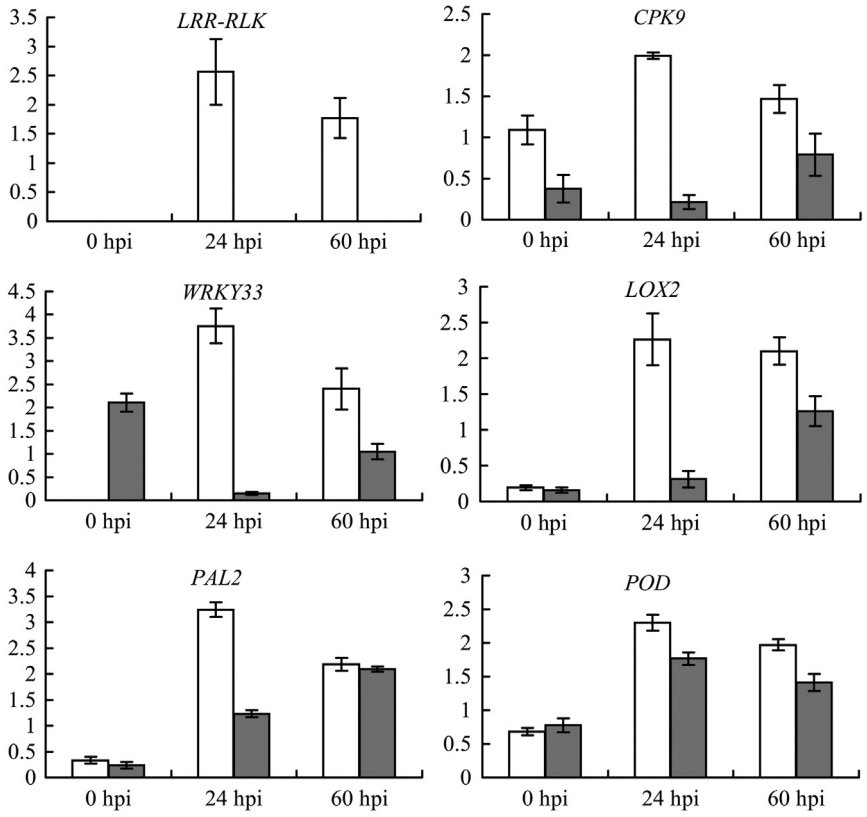

Fig. 5 – Comparison of some defence related gene in *E. urophylla* × *E. tereticornis* M1 (white) and *E. grandis* No.5 (black). The relative expression levels in *E. urophylla* × *E. tereticornis* M1 and *E. grandis* No.5 at 0 hpi, 24 hpi and 60 hpi were obtained by qRT-PCR using the $2^{-\Delta\Delta CT}$ method. Bars represent mean ± SE (n = 6). *LRR-RLK*, Leucine-rich repeat transmembrane protein kinase; *CPK9*, calmodulin-domain protein kinase 9; *WRKY33*, WRKY DNA-binding protein 33; *LOX2*, lipoxygenase 2; *PAL2*, phenylalanine ammonia-lyase 2; *POD*, Peroxidase superfamily protein.

resistance to necrotrophic pathogens [47]. The expression of *AtWRKY33* can be induced rapidly by various biotrophic and necrotrophic pathogens, including *Hyaloperonospora parasitica*, *A. brassicicola*, *A. alternata*, *Sclerotinia sclerotiorum*, and *Pythium sylvaticum* [48]. Additionally, ectopic over-expression of *WRKY33* increased the resistance of *Arabidopsis* to *Botrytis cinerea* and *A. brassicicola* [49]. qRT-PCR showed that *WRKY 33* was significantly up-regulated in the resistant clone, but supressed in the susceptible clone after inoculated with *Calonectria* (Fig. 5). The present results indicated that WRKY 33 may participate in the defense respond of *Eucalyptus* to *C. pseudoreteaudii*.

It was here observed that one sugar transporter and two cell wall invertases (CWI) were up-regulated. Sugar transporters including monosaccharides and disaccharides, participate in both membrane transport and in long-distance sugar transport [50]. CWI can cleave sucrose into glucose and fructose and is considered as a PR protein [51,52]. Genes encoding sugar transporters and CWI can be induced by various stresses in different plant species. They cause the accumulation of hexose, which can enhance the resistance to stresses by providing energy, increasing osmotic pressure, or serving as a signaling molecules in the activation of genes involved in defense mechanisms [53,54].

Trehalose, a non-reducing sugar, has been reported to induce partial resistance to powdery mildew (*Blumeria graminis* f. sp. *tritici*) in wheat by activation of phenylalanine ammonia-lyase and peroxidase genes [55,56]. Singh et al. showed that trehalose is essential to *Arabidopsis thaliana* defense against the green peach aphid [57]. The present results showed the trehalose phosphatase/synthase 11 (TPS11) gene to be up-regulated. This is consistent with the observation that the expression of a putative *TPS11* gene increased in *Arabidopsis* plants infected with *Tobacco mosaic virus* [58].

Environmental stresses can interfere with protein folding and oligomerization and lead to the accumulation and aggregation of unfolded proteins in the endoplasmic reticulum (ER) [59–61]. Then a self-protective signaling pathway called unfolded protein response (UPR) is activated. It induces the expression of molecular chaperones such as BiP and calnexin [62]. These molecular chaperones can help proteins fold accurately and so support normal physiological activities. Calnexin, a highly conserved ER transmembrane protein, plays a crucial role in the folding and quality control of newly synthesized proteins. Several reports have indicated that gene encoding calnexin is up-regulated under various stress conditions [63–65]. The up-regulation of calnexin in *E. urophylla* × *E. tereticornis* M1 demonstrated that it may participate in the response to *Ca. pseudoreteaudii*.

4.2. Signal transduction

Jasmonic acid (JA) and its derivatives play an important role in the regulation of plant defense. It has been reported that genes involved in JA synthesis and the JA signaling pathway are highly expressed in plants under various stresses. This can lead to rapid accumulation of JA, which acts as an intracellular signal transducer and triggers the transcription of defense genes [66,67].

In *C. pseudoreteaudii*-inoculated *Eucalyptus*, proteins key to JA biosynthesis [three lipoxygenase (LOX) and one allene oxide synthase (AOS)] were up-regulated. qRT-PCR results also indicated that transcript abundance of *LOX* (Eucgr.J00821.1) reached a peak more early in the resistant clone than in the susceptible clone, and was always higher than in the susceptible clone after inoculation with *Calonectria* (Fig. 5). Other reports similarly showed that the abundance of *LOX* and *AOS* increased upon attack by pathogen [66,68,69]. Furthermore, overexpression of a gene encoding allene oxide synthase in rice increased levels of endogenous JA as well as expression of the PR gene, finally leading to host resistance to fungal infection [70]. However, it was also found that the transcription amplitude of the gene encoding jasmonate ZIM-domain, which is a negative regulator of the JA signaling pathway, was higher in *E. grandis* × *E. urophylla* 9224 after infection by *C. quinqueseptatum* than at other times. The present work demonstrated that *C. pseudoreteaudii* infection could enhance the biosynthesis of JA and activate the JA pathway in *E. urophylla* × *E. tereticornis* M1.

Reversible phosphorylation of proteins is important in the regulation of plant defense against environmental stresses [71,72]. A previous study has also shown that a gene encoding tyrosine phosphatase in *E. grandis* × *E. urophylla* 9224 was up-regulated during infection by *C. quinqueseptatum* [14]. In this study, two protein kinases involved in phosphorylation, calcium dependent protein kinase (CPK, Eucgr.F00761.1), and leucine-rich repeat transmembrane protein kinase (LRR-RLK, Eucgr.F01306.1), were up-regulated. qRT-PCR data displayed that *CPK* (Eucgr.F00761.1) was always more abundant in the resistant clone than in the susceptible after infection with *Calonectria* (Fig. 5). Evidence showed that CPK is a crucial player in activating the immune reactions of plants, such as the synthesis of ROS, changes in phytohormone synthesis and signaling, and cell death [73,74]. LRR-RLK, a membrane localized receptor-like kinase, has been found to trigger basal defense or MAMP-triggered immunity to protect plants from pathogen infection through conserved microbial-associated molecular patterns (MAMPs) [75]. To date, several RLKs have been reported to be involved in the interactions between plants and microorganisms [76]. Interestingly, qRT-PCR results also showed that *LRR-RLK* (Eucgr.F00761.1) was significantly up-regulated in *E. urophylla* × *E. tereticornis* M1, but couldn't be detected in the susceptible clone *E. grandis* N0.5 after the inoculation with *C. pseudoreteaudii* (Fig. 5). It implied that this gene may act a crucial role in mediating the response of *Eucalyptus* to *C. pseudoreteaudii*.

4.3. Cell transport

Most of the genes involved in cell transport were up-regulated in *E. urophylla* × *E. tereticornis* M1 after the inoculation with *C. pseudoreteaudii*. In plants, the plasma membrane (PM) H^+-ATPases is a key mediator of membrane transport processes. And the mitochondrial ADP/ATP carrier could provide the cytosol with ATP producing by oxidative phosphorylation. The high levels of expression of PM H^+-ATPases and ADP/ATP carrier suggested that these enzymes may be important for the earliest cellular responses to the invasion of *C. pseudoreteaudii*.

4.4. Carbohydrate and energy metabolism

It has been reported that the reprogramming of resourses in plants infected with pathogens may repress photosynthesis, but increased the expression of defence related genes and the produciton of protective compounds [77,78]. This study supported these findings because most of the genes related to photosynthesis in *E. urophylla* × *E. tereticornis* M1 were down-regulated after infection with *C. pseudoreteaudii*, while genes involved in respiration were up-regulated.

4.5. Nucleic acid metabolism

Four RNA binding proteins and two histones were down-regulated, indicating that the metabolism of nucleic acid of *E. urophylla* × *E. tereticornis* M1 was affected by *C. pseudoreteaudii* infection. Cytidine deaminase, which catalyzes the irreversible hydrolytic deamination of cytidine to uridine, was up-regulated [79]. The same study also showed that the gene encoding cytidine deaminase (*Os07g0245100*) was significantly up-regulated after infection with *Magnaporthe oryzae*.

4.6. Protein metabolism

Most of the differentially expressed ribosomal proteins, which make up the ribosomal subunits involved in the translation process, were down-regulated in *E. urophylla* × *E. tereticornis* M1. However, several other proteins involved in protein metabolism were found to be up-regulated, including Ribosomal protein L16p/L10e family protein glutamate decarboxylase (GAD), phosphoserine aminotransferase (PSAT), serine hydroxymethyltransferase (SHMT), and serine carboxypeptidase (SCL). This demonstrated that *C. pseudoreteaudii* infection could impair protein degradation and protein biosynthesis.

The enzyme GAD catalyzes the decarboxylation of glutamate to γ-aminobutyric acid (GABA) and CO_2. GABA has been reported to accumulate under a variety of stress conditions [80]. GAD and GABA transaminase in tomato (*Lycopersicon esculentum* var *commune* Bailey) were induced by *Cladosporium fulvum*. As a result, the concentration of GABA in the apoplast increased from about 0.8 mM to 2-3 M [81,82].

PSAT and SHMT act in the one-carbon compound metabolic pathway. PSAT is involved in the biosynthesis of serine, and SHMT is responsible for interconversion of serine and glycine. Recently, a soybean gene, *Rhg4*, encoding a serine hydroxymethyltransferase, was confirmed to confer resistance on the soybean cultivar (cv.) Forrest against soybean cyst nematode (SCN) [83].

In plants, SCL and serine carboxypeptidase-like proteins (SCPLs) have been reported to act in proteolysis, C-terminal processing, wound response, xenobiotic metabolism, and

secondary metabolism [84]. Moreover, it has been suggested that an increase in the transcription of a rice SCPL gene (*OsBISCPL1*) may play an important role in disease resistance [85]. Because it was induced during an incompatible interaction with the blast fungus *Magnaporthe grisea*, it was able to enhance the resistance of *OsBISCPL1*-overexpressing transgenic *Arabidopsis* plants against *A. brassicicola* and *Pseudomonas syringae* pv. *tomato*.

5. Conclusion

In this study, comparative proteome and transcriptome analyses of *E. urophylla* × *E. tereticornis* M1 infected with *C. pseudoreteaudii* were performed by iTRAQ and RNA-seq techniques. This is the first attempt to survey the response of *Eucalyptus* to *Calonectria sp.* at the protein level. This study showed significant changes in the shikimate/phenylpropanoid pathway, terpenoid biosynthesis, signaling pathway (JA and trehalose), and other defense responses (PR-proteins). Further changes were observed in carbohydrate and energy metabolism, nucleic acid metabolism, and protein metabolism. It was hypothesized that *Eucalyptus* might perceive the invading of *Calonectria sp.*by plant receptors such as LRR-RLK, and quickly trigger multiple signaling pathways that depend on JA and sugar. It led to some defense responses in *Eucalyptus* including the strengthening of cell walls, biosynthesis of PR-proteins and production of other antimicrobial compounds, etc. These downstream defense responses caused a demand for carbohydrates and energy, which became satisfied through reinforcement of the respiration metabolism and the transport of metabolites. The knowledge of host response to pathogen could help to unravel its resistant processes and facilitate the development better control strategies to manage the disease.

Supplementary data to this article can be found online at http://dx.doi.org/10.1016/j.jprot.2014.12.008.

Conflict of interest

The authors declare that no conflict of interest exists in the submission of this manuscript, and manuscript is approved by all authors for publication. This article does not infringe on any copyright or other proprietary right of any third party and was original research that has not been published previously, and not under consideration for publication elsewhere, in whole or in part. All the authors listed have approved the manuscript that is enclosed.

Acknowledgements

We are grateful to Prof. Lu Guodong of College of Plant Protection, Fujian Agriculture and Forestry University, for his valuable advice and technical support. We also thank '*LetPub*' for its linguistic assistance during the preparation of this manuscript. This work was funded by the Project of Financial Department of Fujian Province (No. K8112004a and SCZ10038) and the Natural Science Foundation of Fujian Province (No. 2013 J01074).

REFERENCES

[1] Wingfield MJ, Slippers B, Hurley BP, Coutinho TA, Wingfield BD, Roux J. Eucalypt pests and diseases: growing threats to plantation productivity. Southern Forests. J For Sci 2008;70:139–44.
[2] Zhou XD, Xie YJ, Chen SF, Wingfield MJ. Diseases of *eucalypt* plantations in China: challenges and opportunities. Fungal Divers 2008;32:1–7.
[3] Chen QZ, Guo WS, Feng LZ, Miao SH, Lin JS. Identification of *Calonectria* associated with *Eucalyptus* spp. cutting seedling leaf blight. J Fujian Agric For Univ 2013;42:257–62.
[4] Chen QZ, Guo WS, Ye XZ, Huang XP, Wu YZ. Identification of *Calonectria* associated with *Eucalyptus* leaf blight in Fujian Province. J Fujian For Coll 2013;32:176–82.
[5] Chen SF, Lombard L, Roux J, Xie YJ, Wingfield MJ, Zhou XD. Novel species of *Calonectria* associated with *Eucalyptus* leaf blight in Southeast China. Persoonia 2011;26:1–12.
[6] Zhu JH, Guo WS, Chen HM, Wu JQ, Chen QZ, Meng XM. Loss estimation of *eucalyptus* growth caused by of eucalyptus dieback. For Pest Dis 2011;30:6–10.
[7] Chen QZ. Measurement on the resistance of *Eucalyptus* cultivar to *Cylindrocladium quinqueseptatum*. J Fujian For Coll 2010;30:297–9.
[8] Feng LZ. Relationship between chlorophyll contents and resistance to *Cylindrocladium quinqueseptatum* in *Eucalyptus*. J Fujian Agric For Univ 2008;37:365–8.
[9] Feng LZ, Chen QZ, Guo WS, Su LY, Zhu JH. Relationship between *Eucalyptus* resistance to dieback and secondary metabolism. Chin J Eco-Agric 2008;16:426–30.
[10] Feng LZ, Chen QZ, Guo WS, Zhu JH, Chen HM. Relationship between *Eucalyptus* resistance to *Eucalyptus* dieback and defense enzyme system. Chin J Eco-Agric 2008;16:426–30.
[11] Feng LZ, Huang RH, Guo WS. Relationship between the leaf stomatal characteristics of *Eucalyptus* and their resistance to dieback. J Fujian For Coll 2009;29:293–6.
[12] Feng LZ, Liu YB, Guo SZ, Huang RH, Guo WS. Relationship between the leaf anatomical characteristics of *Eucalyptus* and its resistance to dieback. J Chin Electron Microsc Soc 2008;27:229–34.
[13] Luo JT, Xue ZN, Liao WJ, Yan CL, Ouyang JY, Shan Y. Investigation on the diseases in fast growing *Eucalyptus* spp. in Guangxi. For Pest Dis 2012;31:21–4.
[14] Feng LZ, Guo WS, Xie WF, Chen QZ, Ye XZ. Construction and analysis of a SSH cDNA library of *Eucalyptus grandis* × *Eucalyptus urophylla* 9224 induced by *Cylindrocladium quinqueseptatum*. Botany 2012;90:1277–83.
[15] Thumma BR, Sharma N, Southerton SG. Transcriptome sequencing of *Eucalyptus camaldulensis* seedlings subjected to water stress reveals functional single nucleotide polymorphisms and genes under selection. BMC Genomics 2012;13:364.
[16] Ross PL, Huang YN, Marchese JN, Williamson B, Parker K, Hattan S, et al. Multiplexed protein quantitation in *Saccharomyces cerevisiae* using amine-reactive isobaric tagging reagents. Mol Cell Proteomics 2004;3:1154–69.
[17] Myburg AA, Grattapaglia D, Tuskan GA, Hellsten U, Hayes RD, Grimwood J, et al. The genome of *Eucalyptus grandis*. Nature 2014;510:356–62.
[18] Sun Q, Zhou G, Cai Y, Fan Y, Zhu X, Liu Y, et al. Transcriptome analysis of stem development in the tumourous stem mustard *Brassica juncea* var. *tumida* Tsen et Lee by RNA sequencing. BMC Plant Biol 2012;12:53.
[19] Yin YL, Yu GJ, Chen YJ, Jiang S, Wang M, Jin YX, et al. Genome-wide transcriptome and proteome analysis on different developmental stages of *Cordyceps militaris*. PLoS One 2012;7:e51853.

[20] Li RQ, Yu C, Li YR, Lam TW, Yiu SM, Kristiansen K, et al. SOAP2: an improved ultrafast tool for short read alignment. Bioinformatics 2009;25:1966–7.
[21] Mortazavi A, Williams BA, McCue K, Schaeffer L, Wold B. Mapping and quantifying mammalian transcriptomes by RNA-Seq. Nat Methods 2008;5:621–8.
[22] Audic S, Claverie JM. The significance of digital gene expression profiles. Genome Res 1997;7:986–95.
[23] Kanehisa M, Goto S. KEGG: kyoto encyclopedia of genes and genomes. Nucleic Acids Res 2000;28:27–30.
[24] Cassan-Wang H, Ma Soler, Yu H, Camargo ELO, Carocha V, Ladouce N, et al. Reference genes for high-throughput quantitative reverse transcription–PCR analysis of gene expression in organs and tissues of *eucalyptus* grown in various environmental conditions. Plant Cell Physiol 2012;53:2101–16.
[25] Livak KJ, Schmittgen TD. Analysis of relative gene expression data using real-time quantitative PCR and the $2^{-\Delta\Delta CT}$ method. Methods 2001;25:402–8.
[26] Yang LT, Qi YP, Lu YB, Guo P, Sang W, Feng H, et al. iTRAQ protein profile analysis of *Citrus sinensis* roots in response to long-term boron-deficiency. J Proteome 2013;93:179–206.
[27] Chen QZ, Guo WS, Feng LZ, Ye XZ, Xie WF, Huang XP, et al. Data for transcriptome and proteome analysis of *Eucalyptus* infected with *Calonectria pseudoreteaudii*. J Proteome 2014 (accepted for publication).
[28] De Cremer K, Mathys J, Vos C, Froenicke L, Michelmore RW, Cammue B, et al. RNAseq-based transcriptome analysis of *Lactuca sativa* infected by the fungal necrotroph *Botrytis cinerea*. Plant Cell Environ 2013;36:1992–2007.
[29] Maeda H, Dudareva N. The shikimate pathway and aromatic amino acid biosynthesis in plants. Annu Rev Plant Biol 2012;63: 73–105.
[30] Steinrücken H, Amrhein N. The herbicide glyphosate is a potent inhibitor of 5-enolpyruvyl-shikimic acid-3-phosphate synthase. Biochem Biophys Res Commun 1980; 94:1207–12.
[31] Shadle GL, Wesley SV, Korth KL, Chen F, Lamb C, Dixon RA. Phenylpropanoid compounds and disease resistance in transgenic tobacco with altered expression of L-phenylalanine ammonia-lyase. Phytochemistry 2003;64: 153–61.
[32] Ritter H, Schulz G. Structural basis for the entrance into the phenylpropanoid metabolism catalyzed by phenylalanine ammonia lyase. Plant Cell Online 2004;16:3426–36.
[33] Howles PA, Sewalt VJH, Paiva NL, Elkind Y, Bate NJ, Lamb C, et al. Overexpression of L-phenylalanine ammonia-lyase in transgenic tobacco plants reveals control points for flux into phenylpropanoid biosynthesis. Plant Physiol 1996;112: 1617–24.
[34] Rohde A, Morreel K, Ralph J, Goeminne G, Hostyn V, De Rycke R, et al. Molecular phenotyping of the pal1 and pal2 mutants of *Arabidopsis thaliana* reveals far-reaching consequences on phenylpropanoid, amino acid, and carbohydrate metabolism. Plant Cell Online 2004;16:2749–71.
[35] JCMeS Moura, Bonine CAV, De Oliveira Fernandes Viana J, Dornelas MC, Mazzafera P. Abiotic and biotic stresses and changes in the lignin content and composition in plants. J Integr Plant Biol 2010;52:360–76.
[36] Ni W, Fahrendorf T, Ballance GM, Lamb CJ, Dixon RA. Stress responses in alfalfa (*Medicago sativa* L.). XX. Transcriptional activation of phenylpropanoid pathway genes in elicitor-induced cell suspension cultures. Plant Mol Biol 1996;30:427–38.
[37] Corea ORA, Ki C, Cardenas CL, Kim S-J, Brewer SE, Patten AM, et al. Arogenate dehydratase isoenzymes profoundly and differentially modulate carbon flux into lignins. J Biol Chem 2012;287:11446–59.
[38] Dixon RA, Paiva NL. Stress-induced phenylpropanoid metabolism. Plant Cell 1995;7:1085–97.
[39] Tohge T, Watanabe M, Hoefgen R, Fernie AR. The evolution of phenylpropanoid metabolism in the green lineage. Crit Rev Biochem Mol Biol 2013;48:123–52.
[40] Yu F, Utsumi R. Diversity, regulation, and genetic manipulation of plant mono-and sesquiterpenoid biosynthesis. Cell Mol Life Sci 2009;66:3043–52.
[41] Nagpal N, Shah G, Arora N, Shri R, Arya Y. Phytochemical and pharmacological aspects of Eucalyptus genus. Int J Pharm Sci Res 2010;1:28–36.
[42] Cui H, Liu HJ, Li XJ. Expression of foreign farnesyl diphosphate synthase gene in transgenic tobacco enhances disease resistance to *Alternaria alternata* in vitro. Acta Agron Sin 2006; 32:817–20.
[43] Barna B, Fodor J, Harrach BD, Pogány M, Király Z. The Janus face of reactive oxygen species in resistance and susceptibility of plants to necrotrophic and biotrophic pathogens. Plant Physiol Biochem 2012;59:37–43.
[44] Dowd C, Wilson IW, McFadden H. Gene expression profile changes in cotton root and hypocotyl tissues in response to infection with *Fusarium oxysporum* f. sp. *vasinfectum*. Mol Plant-Microbe Interact 2004;17:654–67.
[45] Sun H, Kim MK, Pulla RK, Kim YJ, Yang DC. Isolation and expression analysis of a novel major latex-like protein (MLP151) gene from *Panax ginseng*. Mol Biol Rep 2010;37: 2215–22.
[46] Dq Yu, Chen Ch, Zx Chen. Evidence for an important role of WRKY DNA binding proteins in the regulation of *NPR1* gene expression. Plant Cell Online 2001;13:1527–40.
[47] Birkenbihl RP, Diezel C, Somssich IE. Arabidopsis WRKY33 is a key transcriptional regulator of hormonal and metabolic responses toward *Botrytis cinerea* infection. Plant Physiol 2012; 159:266–85.
[48] Lippok B, Birkenbihl RP, Rivory G, Brümmer J, Schmelzer E, Logemann E, et al. Expression of *AtWRKY33* encoding a pathogen-or PAMP-responsive WRKY transcription factor is regulated by a composite DNA motif containing W box elements. Mol Plant Microbe Interact 2007;20:420–9.
[49] Zheng Z, Qamar SA, Chen Z, Mengiste T. *Arabidopsis* WRKY33 transcription factor is required for resistance to necrotrophic fungal pathogens. Plant J 2006;48:592–605.
[50] Lemoine R, La Camera S, Atanassova R, Dédaldéchamp F, Allario T, Pourtau N, et al. Source-to-sink transport of sugar and regulation by environmental factors. Front Plant Sci 2013; 4:1–21.
[51] Roitsch T, Balibrea ME, Hofmann M, Proels R, Sinha AK. Extracellular invertase: key metabolic enzyme and PR protein. J Exp Bot 2003;54:513–24.
[52] Ruan YL, Jin Y, Yang YJ, Li GJ, Boyer JS. Sugar input, metabolism, and signaling mediated by invertase: roles in development, yield potential, and response to drought and heat. Mol Plant 2010;3:942–55.
[53] Moghaddam MRB, Van den Ende W. Sugars and plant innate immunity. J Exp Bot 2012;63:3989–98.
[54] Sun L, Yang DL, Kong Y, Chen Y, Li XZ, Zeng LZ, et al. Sugar homeostasis mediated by cell wall invertase GRAIN INCOMPLETE FILLING 1 (GIF1) plays a role in pre-existing and induced defence in rice. Mol Plant Pathol 2013;15:161–73.
[55] Muchembled J, Anissa L-HS, Grandmougin-Ferjani A, Sancholle M. Changes in lipid composition of *Blumeria graminisf.* sp. *tritici* conidia produced on wheat leaves treated with heptanoyl salicylic acid. Phytochemistry 2006; 67:1104–9.
[56] Reignault P, Cogan A, Muchembled J, Lounes-Hadj Sahraoui A, Durand R, Sancholle M. Trehalose induces resistance to powdery mildew in wheat. New Phytol 2001;149:519–29.
[57] Singh V, Louis J, Ayre BG, Reese JC, Shah J. Trehalose phosphate synthase11-dependent trehalose metabolism promotesArabidopsis thalianadefence against the phloem feeding insect *Myzus persicae*. Plant J 2011;67:94–104.

[58] Golem S, Culver JN. Tobacco mosaic virus induced alterations in the gene expression profile of *Arabidopsis thaliana*. Mol Plant Microbe Interact 2003;16:681–8.
[59] Duffee LE, Boatwright JL, Pacha FH, Shockley JM, Pajerowska-Mukhtar KM, Mukhtar MS. Eukaryotic endoplasmic reticulum stress-sensing mechanisms. Adv Life Sci 2012;2:148–55.
[60] Howell SH. Endoplasmic reticulum stress responses in plants. Annu Rev Plant Biol 2013;64:477–99.
[61] Liu JX, Howell SH. Endoplasmic reticulum protein quality control and its relationship to environmental stress responses in plants. Plant Cell Online 2010;22:2930–42.
[62] Srivastava R, Chen Y, Deng Y, Brandizzi F, Howell SH. Elements proximal to and within the transmembrane domainmediate the organelle-to-organellemovement of bZIP28 under ER stress conditions. Plant J 2012;70:1033–42.
[63] Guérin R, Arseneault G, Dumont S, Rokeach LA. Calnexin is involved in apoptosis induced by endoplasmic reticulum stress in the fission yeast. Mol Biol Cell 2008;19:4404–20.
[64] Li MH, Sun Y, Zhao CM, Sun AQ, Hu XR, Liu J. Cloning and stress expression analysis of calnexin in tomato. J Wuhan Bot Res 2006;24:100–5.
[65] Xing J, Wang FT, An YQ, Guan EX, Lin RM, Feng J, et al. Molecular cloning of wheat calnexin gene *Ta*CNX60.0 and analyzing of its expression. J China Agric Univ 2012;17:20–5.
[66] Thatcher LF, Manners JM, Kazan K. *Fusarium oxysporum* hijacks COI1-mediated jasmonate signaling to promote disease development in *Arabidopsis*. Plant J 2009;58:927–39.
[67] Ziegler J, Keinänen M, Baldwin IT. Herbivore-induced allene oxide synthase transcripts and jasmonic acid in *Nicotiana attenuata*. Phytochemistry 2001;58:729–38.
[68] Akram A, Ongena M, Duby F, Dommes J, Thonart P. Systemic resistance and lipoxygenase-related defence response induced in tomato by *Pseudomonas putida* strain BTP1. BMC Plant Biol 2008;8:113.
[69] Li CY, Deng GM, Yang J, Viljoen A, Jin Y, Kuang RB, et al. Transcriptome profiling of resistant and susceptible Cavendish banana roots following inoculation with *Fusarium oxysporum* f. sp. *cubense* tropical race 4. BMC Genomics 2012;13:374.
[70] Schweizer P, Buchala A, Silverman P, Seskar M, Raskin I, Metraux J-P. Jasmonate-inducible genes are activated in rice by pathogen attack without a concomitant increase in endogenous jasmonic acid levels. Plant Physiol 1997;114:79–88.
[71] Fischer EH. Phosphorylase and the origin of reversible protein phosphorylation. Biol Chem 2010;391:131–7.
[72] Lan P, Li W, Schmidt W. A digital compendium of genes mediating the reversible phosphorylation of proteins in Fe-deficient *Arabidopsis* roots. Front Plant Sci 2013;4.
[73] Boudsocq M, Sheen J. CDPKs in immune and stress signaling. Trends Plant Sci 2013;18:30–40.
[74] Tena G, Boudsocq M, Sheen J. Protein kinase signaling networks in plant innate immunity. Curr Opin Plant Biol 2011;14:519–29.
[75] Tör M, Lotze MT, Holton N. Receptor-mediated signalling in plants: molecular patterns and programmes. J Exp Bot 2009;60:3645–54.
[76] Meritxell A-L, Martina KR, Andreas B, Martin P. Receptor kinase signaling pathways in plant-microbe interactions. Annu Rev Phytopathol 2012;50:451–73.
[77] Milli A, Cecconi D, Bortesi L, Persi A, Rinalducci S, Zamboni A, et al. Proteomic analysis of the compatible interaction between *Vitis vinifera* and *Plasmopara viticola*. J Proteome 2012;75:1284–302.
[78] Cremer KD, Mathys J, Vos C, Lutzfroenicke, Michelmore RW, Cammue BPA, et al. RNAseq-based transcriptome analysis of *Lactuca sativa* infected by the fungal necrotroph *Botrytis cinerea*. Plant Cell Environ 2013;36:1992–2007.
[79] Wang XJ, Kang HX, Liu ZS, Wang GL. Expression analysis of genes encoding deoxycytidine/cytidine deaminases in rice. Chin J Rice Sci 2012;26:261–6.
[80] Bouche N, Fromm H. GABA in plants: just a metabolite? Trends Plant Sci 2004;9:110–5.
[81] Solomon PS, Oliver RP. Evidence that γ-aminobutyric acid is a major nitrogen source during *Cladosporium fulvum* infection of tomato. Planta 2002;214:414–20.
[82] Thomma BPHJ, Bolton MD, Clergeot PH, De Wit PJ. Nitrogen controls in planta expression of *Cladosporium fulvum Avr9* but no other effector genes. Mol Plant Pathol 2006;7:125–30.
[83] Liu S, Kandoth PK, Warren SD, Yeckel G, Heinz R, Alden J, et al. A soybean cyst nematode resistance gene points to a new mechanism of plant resistance to pathogens. Nature 2012;492:256–60.
[84] Wang YH, Zou J, Chen XB. Research progress of plant SCP and SCPL proteins. J Biol 2010;27:72–5.
[85] Liu HZ, Wang XE, Zhang HJ, Yang YY, Ge XC, Song FM. A rice serine carboxypeptidase-like gene *OsBISCPLI* is involved in regulation of defense responses against biotic and oxidative stress. Gene 2008;420:57–65.